Journal of Alloys and Compounds 509 (2011) 8542–8548

Contents lists available at ScienceDirect

Journal of Alloys and Compounds

journal homepage: www.elsevier.com/locate/jallcom

Precipitation phases in the nickel-based superalloy DZ 125 with YSZ/CoCrAlY thermal barrier coating

Tianquan Liang[a,b,c], Hongbo Guo[a,c,*], Hui Peng[a,c], Shengkai Gong[a,c]

[a] School of Materials Science and Engineering, Beihang University, No. 37 Xueyuan Road, Beijing 100191, PR China
[b] School of Materials Science and Engineering, Guangxi University, No. 100 Daxue Road, Nanning 530004, PR China
[c] Beijing Key Laboratory for Advanced Functional Materials and Thin Film Technology, Beihang University, No. 37 Xueyuan Road, Beijing 100191, PR China

ARTICLE INFO

Article history:
Received 4 October 2010
Received in revised form 20 May 2011
Accepted 28 May 2011
Available online 6 June 2011

Keywords:
Interdiffusion
Topologically close-packed (TCP) phase
Secondary reaction zone (SRZ)
Thermal barrier coatings (TBCs)

ABSTRACT

Interdiffusion behavior of the thermal barrier coating (TBC) with the CoCrAlY bond coat (BC) and directionally solidified Ni-based superalloy DZ 125 was investigated. Severe inward-diffusion of Al, Co and Cr from the BC to the superalloy and outward diffusion of Ni and refractory elements such as W from the superalloy occur during annealing at 1050 °C in air. After 100 h annealing, a ~30 μm thick inter-diffusion zone (IDZ) forms between the BC and superalloy, and a ~35 μm thick secondary reaction zone (SRZ) forms beneath the IDZ. The IDZ mainly consists of β phase and γ matrix. Besides, small amount of Ta and Hf containing carbides are also observed in the IDZ. Needle and fine granular topologically close-packed (TCP) phases, characterized as rhombohedral μ phases, are abundant in the SRZ. The formation of SRZ is mainly due to the precipitation of refractory elements such as W and Mo from the γ matrix and β phase. The formation mechanism of SRZ and μ-TCP phase is discussed.

1. Introduction

Ni-based superalloys have been widely used as hot-section parts in turbine engines because of their superior performances including high temperature strength at elevated temperature during service [1–3]. To meet the requirements of an increase of turbine inlet temperature and thermal efficiency in modern advanced gas turbine, thermal barrier coatings (TBCs) have been widely applied onto the surfaces of the gas turbine components by various methods such as plasma spraying and electron beam physical vapor deposition (EB-PVD). The application of TBCs greatly enhances the operating temperature and efficiency of gas turbine, and significantly improves the component durability [4–6]. State-of-the-art TBCs usually consist of PtAl diffusion or MCrAlY overlay bond coat (BC) and ceramic top coat. The metallic bond coat has two types of major functions required for the TBC applications. It improves the bonding between the topcoat and the substrate, and it protects the substrate from oxidation and corrosion. Interdiffusion between the bond coat and underlying substrate inevitably occurs during thermal exposure at high temperature, which results in structure instability and phase transformation in the superalloy. Due to the interdiffusion between the coating and superalloy, secondary reaction zone (SRZ) and detrimental topologically close-packed (TCP) phase form in the superalloy, leading to significant reduction in mechanical properties of the superalloy [7,8].

TCP phases including σ, μ and Laves phases are principally composed of elements such as Ni, Cr, Co, W, Mo and Re. For advanced Ni-based superalloys, especially the second or third generation single crystal superalloys, more addition of refractory elements such as W, Mo and Re to the superalloys, aims to improve their creep or stress rupture strength at high temperature. However, allying these elements increases the possibility for the formation of harmful TCP phase in the superalloy after long-term aging or thermal exposure [9]. It will weaken the effect of solid solution strengthening. It has been shown that for the superalloys containing considerable content of refractory elements σ and μ TCP phases will precipitate after long-term aging [10–15]. The body-centered tetragonal (BCT) σ phase contains high level of Cr, while the rhombohedral μ phase is enriched in W and Mo. The presence of brittle TCP phases results in degradation of the mechanical properties of the superalloy through weakening the solid solution strengthening effect or by providing fracture initiation sites [6,10–16].

Interdiffusion behaviors between the coating and the superalloy have been investigated extensively [6,7,17,18]. The investigations are mainly focused on the interdiffusion behaviors between the Ni-based coatings and Ni-based superalloys, as well as the effects on the mechanical properties of the superalloys [18–22]. Directionally solidified Ni-based superalloy DZ 125 has been widely applied as

* Corresponding author at: School of Materials Science and Engineering, Beihang University, No. 37 Xueyuan Road, Beijing 100191, PR China. Tel.: +86 10 8231 7117; fax: +86 10 8233 8200.
E-mail address: guo.hongbo@buaa.edu.cn (H. Guo).

0925-8388/$ – see front matter © 2011 Elsevier B.V. All rights reserved.
doi:10.1016/j.jallcom.2011.05.102

Table 1
Nominal composition of the superalloy DZ 125 (in wt.%).

Ni	Cr	Co	W	Mo	Al	Ti	Ta	Hf	B
Bal	8.4–9.4	9.5–10.5	6.5–7.5	1.5–2.5	4.8–5.4	0.7–1.2	3.5–4.1	1.2–1.8	0.01–0.02

structural materials in advanced aero engine for gas turbine blades and vanes operating at high temperature [23]. CoCrAlY is a protective coating material and is also usually works as the bond coat material in the TBC system due to its satisfying high-temperature oxidation and hot-corrosion resistance. However, so far little attention has been paid to the inter-diffusion behaviors between the superalloy DZ 125 and the TBCs with the CoCrAlY bond coat.

The objective of the present study is to investigate the interdiffusion behavior between the Ni-based superalloy DZ 125 and the CoCrAlY bond coat in the TBC system and to understand the formation mechanisms of the deleterious precipitates such as TCP phases in the superalloy during annealing at 1050 °C.

2. Experimental procedures

Directionally solidified Ni-based superalloy DZ 125 was used as the substrate material, with the nominal chemical composition listed in Table 1. The coating was deposited onto the (0 0 1) plane of the superalloy fabricated into rectangles of approximately 20 mm × 15 mm × 3 mm. The sample surfaces were finely polished by 800-grit emery paper, followed by ultrasonic bath cleaning in the solution of alcohol and acetone. Thermal barrier coatings consisting of Co–22Cr–9Al–0.2Y (wt.%) bond coats (BC) and 7 wt.% Y_2O_3 partially stabilized ZrO_2 (7YSZ) topcoats (TC) were deposited onto the samples by electron beam physical vapor deposition (EB-PVD). The average thickness of the BC and TC layers were about 35 μm and 65 μm, respectively. Before the deposition of YSZ topcoat, the bond coated samples were first annealed for 4 h at 1050 °C in vacuum to achieve a homogenous microstructure of the CoCrAlY bond coat. Subsequently, the sample surfaces were strengthened by shot-peening. Another heat-treatment of the samples was subsequently performed for 2 h at 1050 °C in vacuum, aiming to form a pre-oxide scale on the bond coat. These procedures were necessary to ensure a superior durability of EB-PVD TBCs and were reported in our previous work [18].

The TBC coated specimens were annealed at 1050 °C in air furnace to investigate the effect of interdiffusion between the bond coat and underlying superalloy substrate on the microstructure stability of the superalloy. All the specimens were cut normal to the (0 0 1) plane. The specimens were mounted in epoxy resin after thermal exposure and sectioned, then finely mechanically wet-polished with silicon carbide paper and rinsed in ultra-pure deionized water for cross-section examination. Observation and quantitative analysis of the coating and the phase in IDZ were carried out by a scanning electron microscope (SEM, QUANTA 600) equipped with energy dispersive spectroscopy (EDS) and back scattering electron (BSE) detector, and by an electron probe micro-analyzer (EPMA, JXA-8100), both operating at 20 kV. Transmission electron microscopy (TEM) specimens were prepared by the following steps: the samples were cut into rectangles (3 mm × 1.5 mm × 1 mm), glued together with topcoat face to face using a M-Bond 610 adhesive, mechanically polished to a thickness of approximately 100 μm, glued onto a Φ3-mm copper ring, dimpled to a thickness less than 30 μm using a D 500i dimple followed by ion milling in a GL-696F argon ion beam thinner operating at 5 kV. Dual ion guns operating at gun-specimen angle of about 10° and a current of 0.2 mA per gun were used. The specimens were examined using a JEM-2100F TEM operating at 200 kV. The chemical composition of the precipitate in SRZ was detected by energy-dispersive X-ray analysis (EDX) on TEM.

The lattice parameters were obtained by measurement and calculation from the selected area diffraction pattern (SADP) of the precipitates, and the following details were revealed [24]: vectors as g_1 and g_2 and their angle θ were obtained from the SADP. The diffraction constant was $k = \lambda L = Rd$ ($k = 0.251$ Å × 600 mm = 15.06 mm Å). The constants of r_2/r_1 and θ were obtained comparing calculating R_2/R_1 and θ with referring to the calibration within the allowable errors of $\Delta R/R \leq 0.04$, $\Delta\theta \leq 2°$ and $\Delta d/d \leq 0.02$. The value d_1/a and then a were obtained. Therefore, vectors of $g_1(h_1, k_1, l_1)$ and $g_2(h_2, k_2, l_2)$, θ, zone axis $B[uvw]$ and the crystallographic group were determined. Other parameters can also be obtained by the corresponding relationships. Each phase is determined by at least three SADPs.

3. Results and discussion

3.1. Microstructural evolution in the interdiffusion zone

Fig. 1a shows the cross-sectional SEM micrograph of the as-deposited TBC coated sample. The YSZ topcoat reveals typical columnar structure and the CoCrAlY bond coat is tightly bonding to the superalloy. A ~5 μm thick interdiffusion zone (IDZ) forms between the BC and the substrate after 6 h annealing at 1050 °C in vacuum, as shown in Fig. 1b. A discontinuous secondary reaction zone (SRZ) with the thickness of ~3 μm forms beneath the IDZ.

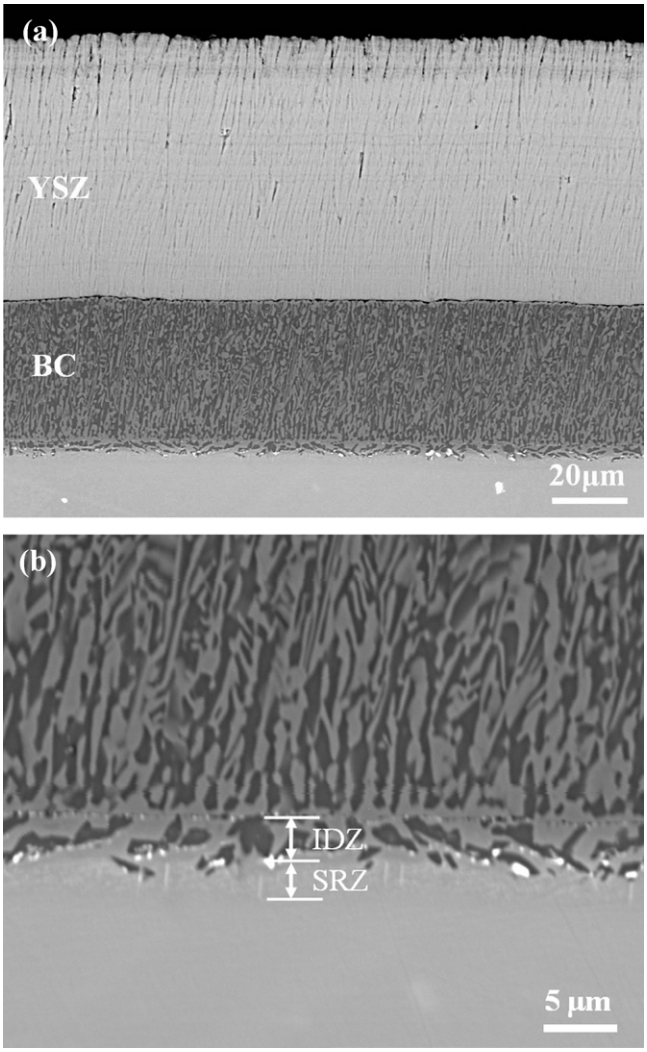

Fig. 1. The cross-sectional micrographs of (a) as-deposited TBC coated superalloy DZ 125, and (b) higher magnification of the local inter-diffusion zone.

The cross-sectional SEM micrograph of the TBC coated sample after 50 h heat-treatment at 1050 °C is shown in Fig. 2. In the bond coat, there is a ~9 μm thick Al depletion zone. A ~25 μm thick IDZ is formed between the bond coat and superalloy substrate. The IDZ basically consists of the γ matrix (light grey) and oblate or bar-like phases (dark). According to the results of EMPA as shown in Table 2, the oblates or bars are determined to be Al-rich β-NiCoAl phases, with the main chemical composition of 53.6 Ni, 21.9 Co, 14.8 Al and 4.9 Cr (wt.%). Besides, small amount of W, Ti, Ta and Hf are also detected in the β phase. In contrast to this, the γ matrix contains more Cr (17.8 wt.%) and Co (35.2 wt.%) but less Al (3.7 wt.%). In addition, some Ta and Hf containing carbides (white) also form in

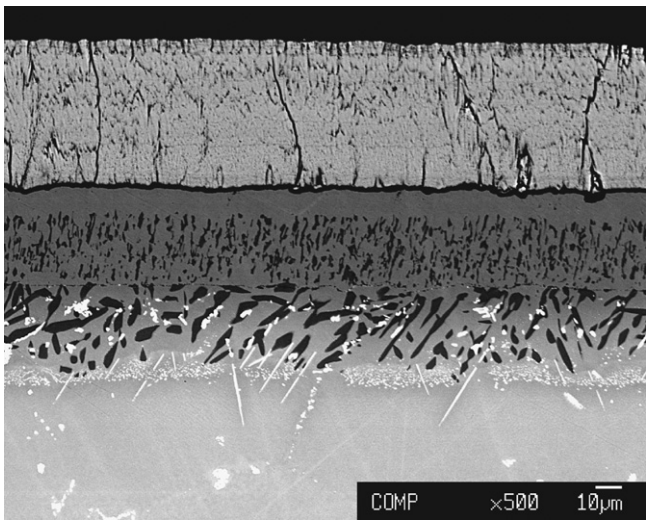

Fig. 2. SEM micrograph of TBC coated superalloy DZ 125 after 50 h annealing at 1050 °C.

the IDZ. Note that there is a ~15 μm thick secondary reaction zone (SRZ) in the superalloy beneath the IDZ after 50 h heat-treatment. Large amount of needle-like phases and finer granular phases are precipitated in the SRZ.

After 100 h heat-treatment, both the Al-depleted zone in the BC and the IDZ do not show apparent increase in thickness (Fig. 3a). However, the SRZ thickness increases to 35 μm, nearly double that of the SRZ after 50 h heat-treatment. At high magnification (Fig. 3b), the needles of ~30 μm in length grows in a preferential orientation normal to the coating/substrate interface [15].

The precipitating granular μ phase is observed mainly along the grain boundary of the β phase at early stage of the interdiffusion. Actually the precipitating phase can be observed after 6 h annealing in vacuum (Fig. 1b). More precipitates appear beneath the IDZ with more formation of β phase when prolonging exposure time at high temperature, and a small amount of needle μ phase forms among the granular ones. The amount of the needle μ phase increases with exposure time as well. The needle phase grows and penetrates into the substrate, and the granular μ phase around the needle phase disappears after long-term thermal exposure (Figs. 2 and 3).

Elements profiles along the thickness of the as-deposited and the annealed specimens are compared in Fig. 4a–f, respectively. The trace to measure the elemental profile is the broken line shown in Fig. 3a. The elemental profile experiment was carried out along the broken line in a step of 7 μm. The concentrations of Al and Co in the bond coat before heat-treatment are about 9 wt.% and 65 wt.%, respectively, while they decrease to less than 6 wt.% and 40 wt.% after a 100 h annealing at 1050 °C. It is obvious that severe inward diffusion of Al and Co occurs during annealing. In contrast to this, the elements Ni, W and Ti from the superalloy substrate diffuse toward the coating surface. As a result, more than 30 Ni, 3 W and 0.2 Ti (wt.%) are present in the bond coat after 100 h annealing. The Cr content in the bond coat slightly reduces after inward diffusion. Note that the peaks of the Ti and Al profiles in the IDZ indicate that the β phase is enriched with these elements (indicated by the arrow in Fig. 3a).

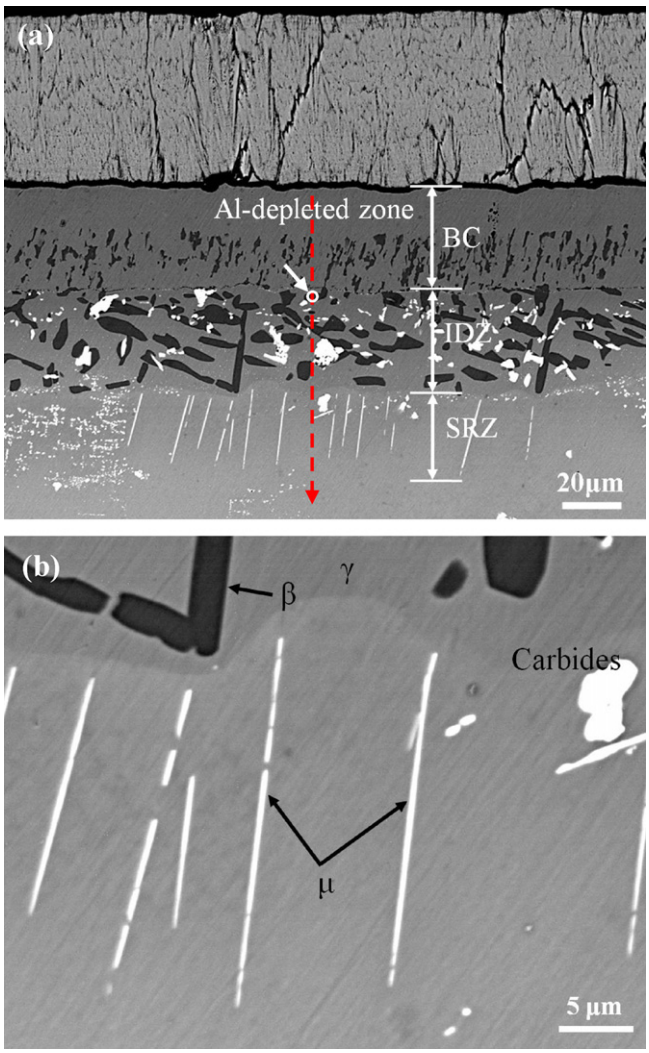

Fig. 3. SEM micrographs of TBC coated superalloy DZ 125 after 100 h annealing at 1050 °C (a) and its higher magnification (b).

Because of Ni depletion, the solid solution elements such as W, Mo, and Ta will segregate to form several complex phases in the IDZ [18,22,25]. The increased contents of Co, Cr, Al and the depletion of Ni in the superalloy will cause the microstructure instability of the γ/γ′ matrix. Due to outward diffusion of refractory elements such as W and Ti, the solid solution strengthening effect of the superalloy can be weakened. On the other hand, the loss of the elements in the bond coat such as Cr and Al will degrade the oxidation and hot-corrosion resistance [26]. Another result is the reduction of the primary γ′/γ matrix and the formation of β phase with low solubility in refractory elements [11]. This results in precipitating of refractory elements from the matrix phases. The refractory elements will segregate and form a layer with abundant refractory phases, namely secondary reaction zone (SRZ) [6].

The thicknesses of the IDZ and SRZ formed in the coated samples after different heat-treatment durations are listed in Table 3. The thickness of IDZ markedly increases with exposure time during

Table 2
Chemical compositions of the β and γ phases in the IDZ of Fig. 3b (in wt.%).

Elements	Al	Cr	Co	Ni	W	Ti	Ta	Hf
β	14.8	5.9	21.9	53.6	1.7	0.6	0.7	0.7
γ	3.7	17.8	35.2	36.7	6.4	0.3	–	–

Table 3
Thickness of IDZ and SRZ as a function of exposure time at 1050 °C.

Time	0 h	20 h	50 h	100 h
IDZ/μm	5	16	25	30
SRZ/μm	3	10	15	35

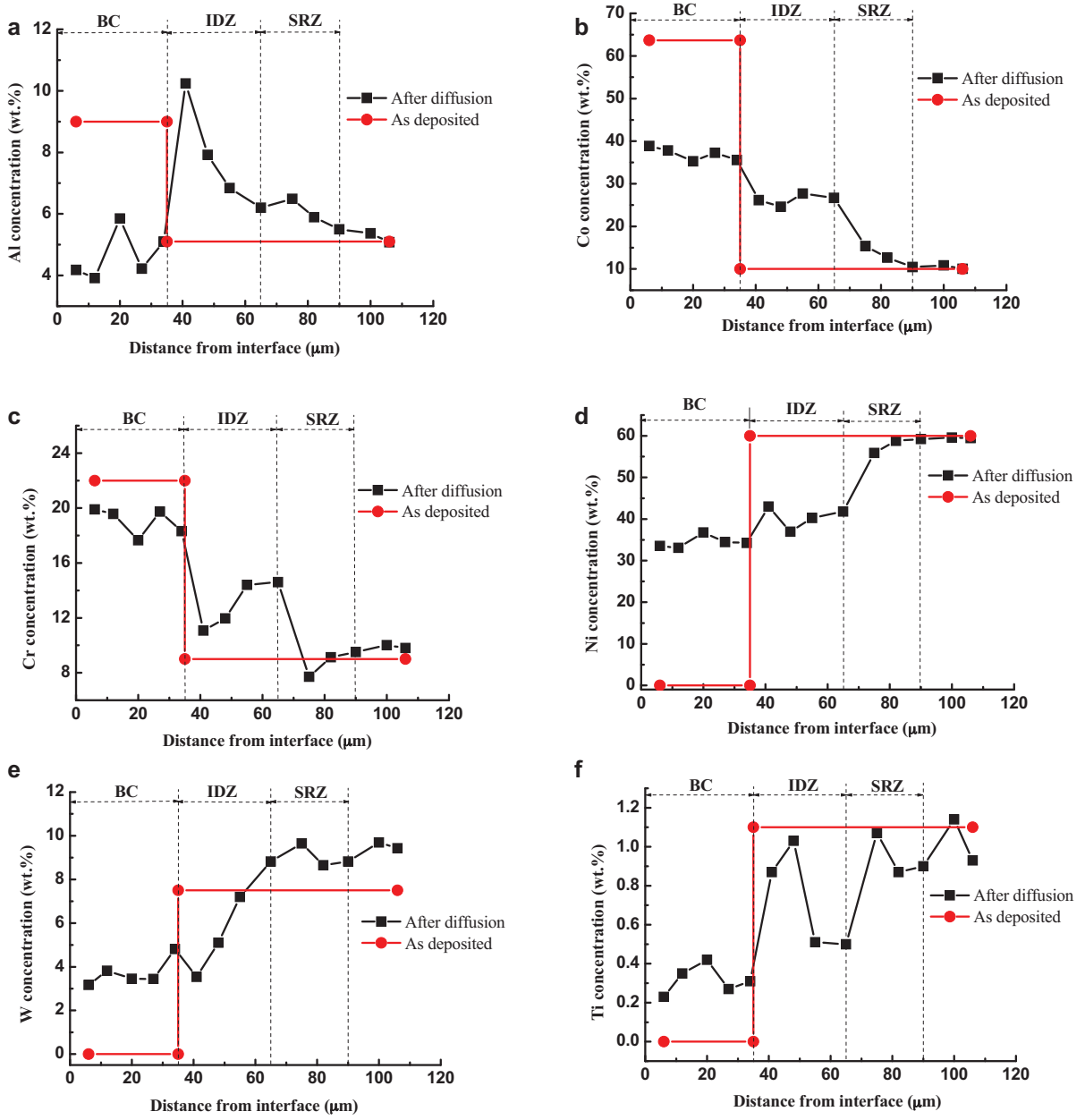

Fig. 4. Element profiles along the thickness of the as-coated specimen and of the specimen annealed for 100 h at 1050 °C.

the first 50 h, but increases slowly in the latter 50 h. The thickness of SRZ is only ~15 μm after the initial 50 h exposure, whereas it increases to ~35 μm after a further 50 h heat-treatment. The thickness of both the IDZ and the SRZ increases with the exposure time. The thickness of the IDZ increases very fast during the initial 50 h while its increment slows down during the later 50 h exposure (Table 3). This is related to the reserve of aluminum in the bond coat. The Al content of the CoCrAlY coating decreases with prolonged exposure time at high temperature, which results in the Al inward-interdiffusion to the substrate is not so significant as that of the initial stage after 50 h owing to the limited Al concentration. The thickness increment of IDZ slows down. Whereas a further severe outward diffusion of nickel still occurs during the later 50 h exposure. This causes the reduction of Ni in IDZ and the microstructure instability of the superalloy. Consequently phase transformations such as $\gamma'\text{-}Ni_3Al + 2[Al] \rightarrow 3\beta\text{-}NiAl$ and $3\gamma\text{-}Ni + [Al] \rightarrow \gamma'\text{-}Ni_3Al$ in the substrate occur, leading to phase instability of γ/γ' matrix. This results in precipitating more refractory elements due to low solubility in β phase and super-saturation in γ phase. More refractory elements will segregate and promote forming μ-TCP phase. Simultaneously the needle μ phase grows and penetrates into the substrate. This results in significant increase of thickness in SRZ during the later 50 h thermal exposure while slight increase of the thickness in IDZ is noticed.

Fig. 5 shows the microstructure of the precipitate in the SRZ of the coated sample after 100 h heat-treatment at 1050 °C. Two types of granular and needle-like precipitates are observed in the SRZ (Fig. 5a and c). The diameter of the granular μ phase is less than 1 μm, while the needles having a small diameter of ~0.4 μm. In view of their selected area electron diffraction (SAD) patterns as shown in Fig. 5b and d, both types of precipitates are determined to have a rhombohedral lattice. The rhombohedral lattice of the precipitates belongs to space group of $D_{3d}^5 - R\bar{3}m$. The lattice constants of the rhombohedral μ phase are $a = 0.477 \pm 0.003$ nm and

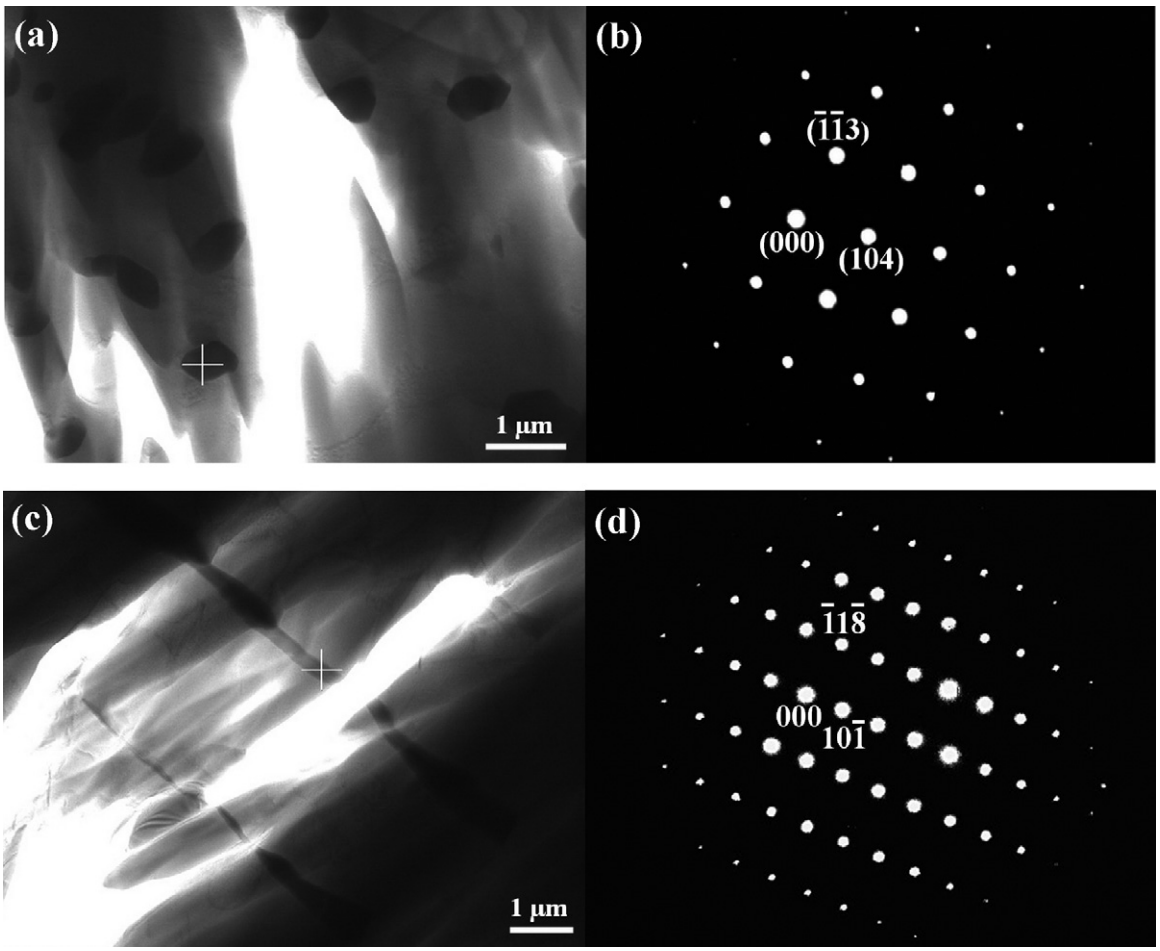

Fig. 5. Microstructure of the precipitation in the SRZ of the coated sample after 100 h annealing at 1050 °C: (a) the granular TCP phase; (b) SADP of the granular phase, $B = [4\ \bar{7}\ \bar{1}]$; (c) the needle-like TCP phase; (d) SADP of the needle phase, $B = [1\,4\,1]$.

$c = 2.585 \pm 0.015$ nm. This is well consistent with the parameters reported by Zheng and Zhang [27].

Due to Ni depletion and the formation of β, the solid solution strengthening elements such as W, Cr, Mo, Hf and Ta segregate in the IDZ and SRZ [6]. The precipitation of the refractory elements in the SRZ promotes the formation of μ phases. Note that the granular phase and needle phase have the similar chemical composition, as shown in Table 4, there are no granular phases near the needle-like ones (Fig. 3a). It can be inferred that the formation of the needle phase is at the expense of the granular phase.

3.2. Diffusion behavior and precipitation mechanism

The morphologies of the β phase in IDZ and μ phases in SRZ are strongly dependent on the diffusion path of the elements in the coated substrate. Elements Al, Co, Cr, Ni, Ti and W will diffuse along different diffusion paths, as shown in Fig. 6, which have significant effect on the morphology of the newly formed phase including β and TCP phases. From the schematic diffusion path, Al from the bond coat and Ni from the superalloy are transferred through the β phase but each in reverse direction, while Co and Cr in the γ matrix of the bond coat diffuse into the superalloy. Simultaneously, W from the superalloy diffuses to the coating. The interdiffusion of elements will alter the original chemical composition in the area of the superalloy close to the coating/superalloy interface, thus resulting in the microstructure instability of the superalloy. The refractory elements segregate from the matrix to form the needle μ phase by consumption of the granular phase through uphill diffusion.

Table 4
Chemical compositions of the μ phases in SRZ of Fig. 5a and c by EDX (wt.%).

Elements	Cr	Co	Ni	W	Mo
Granular	14.5	1.9	4.9	65.2	13.6
Needle	17.7	3.1	7.6	57.8	13.8

The formation of SRZ is closely related to inward-diffusion of Co, Cr, Al from the CoCrAlY bond coat and outward-diffusion of Ni from the underlying superalloy, and is related to the reaction with those elements in the superalloy. The reaction between these elements leads to the formation of the β (NiCoAl) phase. As a result, the superalloy can be changed from the initial γ′/γ to a mixture of γ, β and μ phases owing to the decreased amount of γ′ phase in the IDZ. Simultaneously, the enrichment of Al and depletion of Ni in the IDZ can promote segregation of refractory elements such as W, Cr and Mo and the formation of TCP phases [28–30,17,31].

In this work, the precipitates nucleate from the γ′/γ matrix because of the segregation of W, Co, Cr and Mo at high temperature (Fig. 6), which has also been reported by Proctor [32]. These refractory elements will segregate and become granular or globular under the driving force of chemical potential gradient through uphill diffusion in the SRZ. Finally, the needle μ-TCP phase is developed from the granular phase and grows into the superalloy in the direction normal to the coating/substrate interface.

The formation tendency of the μ-TCP phase in the IDZ of the present superalloy is predicted based on the theory of electron vacancy called PHACOMP [33,34], which has been used to design

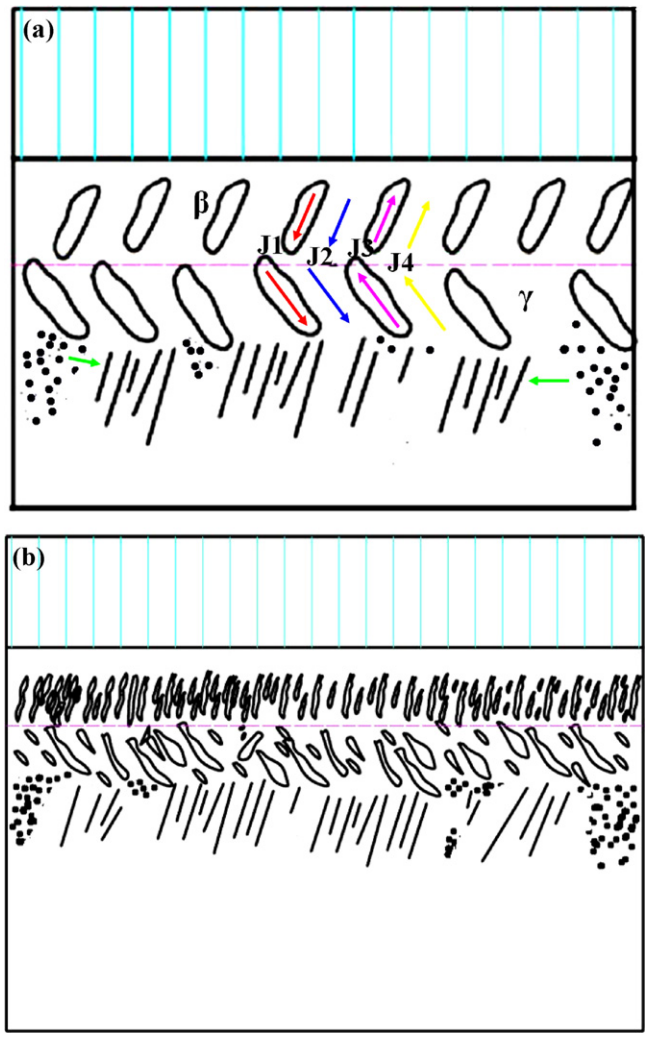

Fig. 6. Schematic of diffusive path of elements (a) formation of IDZ and SRZ (b) after 100 h annealing at 1050 °C. The diffusive fluxes of J_1 to J_4 are representative for Al, Co, Cr, Ni, W and Ti, respectively.

the chemical composition for superalloys. The calculation value for $\overline{N_v}$ and $\overline{M_d}$ can be available by the following equations [35]:

$$\overline{N_v} = \sum_{i=1}^{n} m_i (N_v)_i \quad (1)$$

$$\overline{M_d} = \sum_{i} X_i (M_{d_i}) \quad (2)$$

For Eq. (1), here $\overline{N_v}$ is the number of average electron vacancy; m_i and $(N_v)_i$ are atomic percentage and the electron vacancy number for element i, respectively. For Eq. (2), $\overline{M_d}$ is the average M_d value based on d-electrons alloy theory by New PHACOMP; X_i and M_{d_i} are mol-percentage and the M_d value for element i, respectively.

The critical value of N_v determined by combination of experiments with electron vacancy theory is obtained from Refs. [27,35]. The critical value of M_d is obtained from the experiential equation:

$$M_{d_c} = 6.25 \times 10^{-5} T + 0.834 \quad (3)$$

Here T is Kelvin temperature. The influence of the temperature is considered for the NEWPHACOMP critical value in this equation [35]. The critical numbers N_{v_C} and M_{d_C} in this work are 2.30 and 0.9167 at 1050 °C, respectively.

Table 5
Prediction of μ TCP phase precipitation tendency by N_v and M_d calculations.

Phase	Calculation value		Critical value		Tendency
	$\overline{N_v}$	$\overline{M_d}$	N_{v_C}	M_{d_C}	
β	3.0842	1.1027	2.30	0.9167	Yes
Y	2.4326	0.9368			Yes

According to chemical composition of the present superalloy, the calculation value of $\overline{N_v}$ and $\overline{M_d}$ can be obtained by the following equations based on Eqs. (1) and (2):

$$\overline{N_v} = 7.66\text{Al} + 6.66\text{Ti} + 4.66\text{Cr} + 1.71\text{Co} + 0.61\text{Ni} + 6.66\text{Hf} + 5.66\text{Ta} + 4.66\text{W} + 4.66\text{Mo} \quad (4)$$

$$\overline{M_d} = 1.90\text{Al} + 2.271\text{Ti} + 1.142\text{Cr} + 0.777\text{Co} + 0.717\text{Ni} + 3.020\text{Hf} + 2.224\text{Ta} + 1.655\text{W} + 1.550\text{Mo} \quad (5)$$

The predicted precipitation tendency of TCP phase by N_v and M_d calculation is given in Table 5. Both of the two predominant phases in the IDZ have the tendency of precipitation of TCP phases by the theory of electron vacancy because their $\overline{N_v}$ and $\overline{M_d}$ values are higher than the critical values. Especially for the newly formed β phase, the calculated values ($\overline{N_v}$: 3.0842; $\overline{M_d}$: 1.1027) are much higher than the critical ones (N_{v_C} : 2.30; M_{d_C} : 0.9167) [27,35]. Consequently, it is prone to form the precipitates. Also, the matrix γ phase with $\overline{N_v}$ (2.4326) and $\overline{M_d}$ (0.9368) is prone to precipitate in the IDZ, while the calculated $\overline{N_v}$ value is 2.208 for the very stable superalloy DZ 125 used in this work. This indicates that the formation of body-center cubic β phase with significant precipitation tendency promotes the precipitation of the refractory elements due to its extremely low solubility in the β phase. This is well accordant to the theory of alloy design and experimental results in this work.

The severe interdiffusion between the bond coat and the underlying superalloy has an important impact on the mechanical property of the superalloy and the lifetime of a TBCs system. The inward diffusion of Al and Cr, and the outward diffusion of Ni, Hf, W and Ti will occur during exposure at high temperature. The interdiffusion leads to induce the phase transformation in the IDZ such as γ'-$Ni_3Al + 2[Al] \rightarrow 3\beta$-NiAl and 3γ-$Ni + [Al] \rightarrow \gamma'$-$Ni_3Al$ and causes microstructure instability of the γ/γ' matrix. This promotes precipitating refractory elements such as W and Mo, which results in the further forming μ-TCP phases, and then forms a SRZ beneath the IDZ. On the other hand, the formation of β phase also increases a transverse grain boundary within the directionally solidified superalloy DZ 125. This occurrence will deteriorate the stress rupture performance of the superalloy at high temperature by weakening the effect of solid solution strengthening, formation of transverse grain boundary and TCP phases providing fracture initiation sites [12,35–37]. As well the severe interdiffusion significantly influences the lifetime of a TBCs system [38]. Occurrence of severe inward diffusion of Al and Cr in the bond coat tends to cause depletion of Al and Cr in the bond coat, resulting in phase transformation and the degradation in oxidation and hot corrosion resistance for the bond coat. Although Hf that diffuses from the substrate at the TGO/BC interface is beneficial to the adhesion of the TGO to the bond coat [18,39], the outward-diffusion of the substrate elements such as Ni, Ti and W into the bond coat will be detrimental to the adhesion of TGO–BC owing to forming the spinel and volatile. It damages the integrity of the protective scale at the surface of the bond coat [40].

4. Conclusions

The precipitates in the TBC coated Ni-based directionally solidified superalloy DZ 125 during thermal exposure at 1050 °C are investigated. Significant interdiffusion between the CoCrAlY bond coat and the superalloy DZ 125 occurs during exposure at 1050 °C, resulting in the formation of both the IDZ and the SRZ. The IDZ mainly consists of γ phase, β-NiCoAl phase and Ta and Hf containing carbides, while the SRZ beneath the IDZ are predominantly γ/γ′ matrix and rhombohedral μ TCP phases.

Acknowledgements

This research is sponsored by National Natural Science Foundation of China (NSFC, Nos. 50771009, 50731001 and 51071013) and National Basic Research Program (973 Program) of China under Grant No. 2010CB631200.

References

[1] A. Raffaitin, F. Crabos, E. Andrieux, D. Monceau, Surf. Coat. Technol. 201 (2006) 3829–3835.
[2] C.T. Liu, J. Ma, X.F. Sun, J. Alloys Compd. 491 (2010) 522–526.
[3] G. Liu, L. Liu, C. Ai, B.M. Ge, J. Zhang, H.Z. Fu, J. Alloys Compd. 509 (2011) 5866–5872.
[4] Z.H. Xu, S.M. He, L.M. He, R.D. Mu, G.H. Huang, X.Q. Cao, J. Alloys Compd. 509 (2011) 4273–4283.
[5] X.Y. Xie, H.B. Guo, S.K. Gong, H.B. Xu, Surf. Coat. Technol. 205 (2011) 4291–4298.
[6] D.K. Das, K.S. Murphy, S. Ma, T.M. Pollock, Metall. Mater. Trans. A 39A (2008) 1647–1657.
[7] J. Angenete, K. Stiller, E. Bakchinova, Surf. Coat. Technol. 176 (2004) 272–283.
[8] B. Bai, H. Guo, H. Peng, L.Q. Peng, S.K. Gong, Corros. Sci. (2011) 025, doi:10.1016/j.corsci.2011.04.
[9] R. Rettig, R.F. Singer, Acta Mater. 59 (2011) 317–327.
[10] J.X. Yang, Q. Zheng, X.F. Sun, H.R. Guan, Z.Q. Hu, Mater. Sci. Eng. A 465 (2007) 100–108.
[11] K.Y. Cheng, C.Y. Jo, T. Jin, Z.Q. Hu, J. Alloys Compd. (2011) 001, doi:10.1016/j.jallcom.2011.04.
[12] V.D. Divya, U. Ramamurty, A. Paul, Intermetallics 18 (2010) 259–266.
[13] H. Murakami, T. Sakai, Scripta Mater. 59 (2008) 428–431.
[14] J.-B. le Graverend, J. Cormier, P. Caron, S. Kruch, F. Gallerneau, J. Mendez, Mater. Sci. Eng. A 528 (2011) 2620–2634.
[15] J.X. Yang, Q. Zheng, X.F. Sun, H.R. Guan, Z.Q. Hu, Scripta Mater. 55 (2006) 331–334.
[16] F. Long, Y.S. Yoo, C.Y. Jo, S.M. Seo, H.W. Jeong, Y.S. Song, T. Jin, Z.Q. Hu, J. Alloys Compd. 478 (2009) 181–187.
[17] J. Angenete, K. Stiller, Mater. Sci. Eng. A 316 (2001) 182–194.
[18] H. Peng, H.B. Guo, J. He, S.K. Gong, J. Alloys Compd. 502 (2010) 411–416.
[19] Kh. Rahmani, S. Nategh, Mater. Sci. Eng. A 486 (2008) 686–695.
[20] H. Wei, H.Y. Zhang, X.F. Sun, M.S. Dargusch, X. Yao, J. Alloys Compd. 493 (2010) 507–516.
[21] S.G. Tian, M.G. Wang, T. Li, B.J. Qian, J. Xie, Mater. Sci. Eng. A 527 (2010) 5444–5451.
[22] H.X. Chen, K.S. Zhou, Z.P. Jin, C.L. Liu, J. Therm. Spray Technol. 13 (2004) 515–520.
[23] C.S. Wang, J. Zhang, L. Liu, H.Z. Fu, J. Alloys Compd. 508 (2010) 440–445.
[24] D.B. Williams, C.B. Carter, Transmission Electron Microscopy: A Textbook for Materials Science, Springer, New York, 1996, p. 271.
[25] H.B. Guo, Y.J. Cui, H. Peng, S.K. Gong, Corros. Sci. 52 (2010) 1440–1446.
[26] H.M. Tawancy, N. Sridhar, N.M. Abbas, J. Mater. Sci. 35 (2000) 3615–3629.
[27] Y.R. Zheng, D.T. Zhang, Color Metallographic Investigation of Superalloys and Steels, National Defence Industry Publishers, Beijing, 1999, p. 198.
[28] J. Angenete, K. Stiller, Surf. Coat. Technol. 150 (2002) 107–118.
[29] E. Basuki, A. Crosky, B. Gleeson, Mater. Sci. Eng. A 224 (1997) 27–32.
[30] Y.H. Kong, Q.Z. Chen, Mater. Sci. Eng. A 366 (2004) 135–143.
[31] Y. Wang, H.B. Guo, H. Peng, L.Q. Peng, S.K. Gong, Intermetallics 19 (2011) 191–195.
[32] C.S. Proctor, Ph.D. Thesis, Department of Materials Science and Metallurgy, University of Cambridge, New York, USA, 1994.
[33] S.H. Mousavi Anijdan, A. Bahrami, Mater. Sci. Eng. A 396 (2005) 138–142.
[34] B. Seiser, R. Drautz, D.G. Pettifor, Acta Mater. 59 (2011) 749–763.
[35] J.T. Guo, Materials Science and Engineering for Superalloys, Vol. 1, Sci. Press, Beijing, 2008, p. 716.
[36] W.Z. Li, Y.Q. Li, C. Sun, Z.L. Hu, T.Q. Liang, W.Q. Lai, J. Alloys Compd. 506 (2010) 77–84.
[37] W.Y. Ma, Ph.D. thesis, School of Materials Science and Technology, Beihang University, Beijing, China, 2007, p. 121.
[38] T.Q. Liang, H.B. Guo, H. Peng, S.K. Gong, Surf. Coat. Technol. 205 (2011) 4374–4379.
[39] U. Schulz, M. Menzebach, C. Leyens, Y.Q. Yang, Surf. Coat. Technol. 146–147 (2001) 117–123.
[40] U. Schulz, F. Klaus, E.S. Andrea, Surf. Coat. Technol. 203 (2008) 449–455.